

Mechanical Properties of CRETE, a Polyurethane Foam

S. H. GOODS,¹ C. L. NEUSCHWANGER,² C. C. HENDERSON,² D. M. SKALA²

¹ Materials Reliability Department, 8712, Sandia National Laboratories, P.O. Box 969, Livermore, California 94551-0969

² Polymer and Electrochemical Technologies Department, 8230, Sandia National Laboratories, P.O. Box 969, Livermore, California 94551-0969

Received 15 July 1997; accepted 29 September 1997

ABSTRACT: The room-temperature mechanical properties of a closed-cell, polyurethane encapsulant foam were measured as a function of foam density. Over the range of densities examined, the modulus could be described by a power-law relationship with respect to density. This power-law relationship was the same for both tension and compression testing. The basis for this power-law relationship is explained in terms of the elastic compliance of the cellular structure of the foam using a simple geometric model put forth by Gibson and Ashby. The elastic collapse stress, a property relevant to compression testing, also is found to exhibit a power-law relationship with respect to density. The density dependence of this property is also found in the work of Gibson and Ashby and is explained in terms of the Euler buckling of the struts that comprise the cellular structure. Energy absorption during deformation is also reported for both tension and compression testing. © 1998 John Wiley & Sons, Inc.* J Appl Polym Sci 68: 1045–1055, 1998

Key words: foam; mechanical properties; modulus; collapse stress; energy absorption

INTRODUCTION

Polyurethane foams are used as encapsulants to provide environmental isolation and to mitigate harsh thermal and mechanical shock environments. For the latter application, it is necessary to fully characterize the tension and compression properties of the chosen foam system. Compression properties are especially important for mechanical shock applications as the encapsulant will invariably be required to withstand compressive mechanical loads.

Historically, a principal constituent of many polyurethane foam systems has been toluene diisocyanate (TDI), a suspect human carcinogen.

The United States Department of Energy has directed that attempts be made to replace materials containing such suspected carcinogens within its network of laboratories. To that end, the CRETE foam system, which uses non-TDI constituents, was developed and is the subject of the work reported here. The purpose of the current work was twofold. Our first goal was to measure the “quasi-static” tensile and compressive mechanical properties of CRETE, specifically, the elastic modulus, compressive collapse stress, and tensile and compressive energy absorption. A second goal was to relate certain of these properties to the microstructure and density of the foam through simple microstructural models based on cell strut flexure and buckling.

EXPERIMENTAL

Formulation of the CRETE Foam System

CRETE is a rigid, closed-cell, water-blown polyurethane foam formulated from the following constituents:

Correspondence to: S. H. Goods.

Contract grant sponsor: DOE; contract grant number: DE-AC04-94AL85000.

Journal of Applied Polymer Science, Vol. 68, 1045–1055 (1998)
© 1998 John Wiley & Sons, Inc. *This article is a U.S. Government work and, as such, is in the public domain in the United States of America.

CCC 0021-8995/98/071045-11

- Voranol 490: A poly(ether polyol), made from poly(propylene oxide) and a sucrose/glycerin base, available from Dow Chemical (Midland, MI). The manufacturer specifies the following properties: density (25°C), 0.11 kg/cm³; typical hydroxyl number, 490 mg KOH equiv/g of resin; functionality, 4.3 (calculated); average molecular weight, 460 g/mol; and viscosity (25°C), 5572 cps.
- DC193: A silicone glycol copolymer surfactant from Air Products (Allentown, PA) with an average hydroxyl number of 75.
- Polycat 17: A tertiary amine catalyst (trimethyl-*N*-hydroxyethyl propylene diamine) available from Air Products with an average hydroxyl number of 400.
- Distilled water: Added in various amounts as a chemical blowing agent producing carbon dioxide.
- Isonate 143L: A modified methylene diisocyanate (MMDI) available from Dow Chemical. The manufacturer specifies the following properties for Isonate 143L: isocyanate equivalent weight, 144.5 g; NCO content by weight, 29.2%; functionality, 2.1; viscosity (25°C), 33 cps.

As with other polyurethane foams, the reaction of the water with isocyanate produces carbon dioxide that expands the foam. No physical blowing agents are used. The density of the CRETE foam system is varied by changing the amount of added water, thereby controlling the amount of rise in the foam. The amount of the catalyst and surfactant are also slightly varied to optimize the processing and foam properties.

Examples of some, but not all, of the actual formulations used in the present work are shown in Table I. The free-rise density is measured for a 100-g sample poured from a 200-g batch of CRETE foam expanding in a 500-mL polyethylene container. The free-rise density depends on the temperature of the reaction and thus will vary slightly depending on the size of the batch.

Processing of the CRETE Foam System

Samples of the CRETE foam were generated by the addition of the isocyanate component (Isonate 143L) to the polyol component premixed with DC193, Polycat 17, and water. The resulting reaction mixtures were stirred at 1500 rpm for 60 s using a Conn mixing blade (51-mm diameter).

The mixed products were then poured into cylindrical molds at room temperature. The molds were lightly waxed with a nonsilicone mold release. The molds were then closed, and the foam was allowed to expand to fill the closed molds at a packed density approximately 1.75 times the expected free-rise density. This packed density is also reported in Table I.

The reaction times for the CRETE system were generally less than 8 min from the time of complete mixing. The samples were postcured in an oven for a minimum of 8 h at 66°C. Right circular samples of the foam were cored from the molded samples with the cylinder axis parallel to the direction of the foam rise. None of the core samples included the foam skin or any material within 3 mm of the skin. The density of each foam core was measured and was usually slightly less than the density of the entire sample including the foam skin. These cored samples were used in the mechanical testing reported below.

Mechanical Testing

Room-temperature uniaxial tension and compression mechanical properties were evaluated as a function of foam density using a conventional Instron mechanical test frame. Most tests were conducted at an initial strain rate of $1.7 \times 10^{-4} \text{ s}^{-1}$. Some tests were run at rates between 1.7×10^{-5} and $1.7 \times 10^{-2} \text{ s}^{-1}$ in order to examine the strain-rate effects. All specimens were instrumented with a mechanically attached extensometer for displacement measurement. Tension and compression specimens are shown in Figure 1. The tension specimens had a gauge length of 25.4 mm and a reduced gauge diameter of 19.0 mm and were bonded to steel pull studs. The reduced gauge section ensured that failure occurred within the specimen between the attachment points of the extensometer and not at the bond line between the foam and the pull studs. The compression specimens were simple, right circular cylinders 50.8 mm long and 28.7 mm in diameter.

The mechanical properties were measured for foam densities between 0.12 and approximately 0.60 g/cm³. For tension testing, the modulus (E^*),[†] ultimate tensile strength (UTS), and energy absorption/unit volume (toughness) were

[†] Terms or values annotated by “*” refer to parameters of the foam; other terms annotated by “s” refer to parameters related to the solid polymer.

Table I Selected Formulations for Foam Specimens

Formulations	Packed Density (g/cm ³)				
	0.17	0.22	0.28	0.34	0.42
	Expected Free-Rise Density (g/cm ³)				
	0.10	0.13	0.16	0.19	0.24
Voranol 490	100 phr ^a	100 phr	100 phr	100 phr	100 phr
DC193	2.53 phr	2.45 phr	2.05 phr	1.90 phr	1.73 phr
Polycat 17	0.50 phr	0.47 phr	0.49 phr	0.54 phr	0.63 phr
Water	1.15 phr	0.78 phr	0.58 phr	0.46 phr	0.34 phr
Isonate 143L	152.2 phr	146.0 phr	142.6 phr	140.5 phr	138.0 phr

^a Parts per hundred resin.

measured. The latter parameter was calculated as the area under the tensile stress–strain curve (see Fig. 2). For compression testing where macroscopic fracture did not occur, tests were run to engineering strains of approximately 0.3 (30%). Strength and energy absorption at 0.1 (10%) strain were recorded for comparison. An additional parameter for compression testing, the elastic collapse stress, σ_{el}^* , a broad plateau region subsequent to linear loading, was also measured.

RESULTS AND DISCUSSION

Tension

Figure 3 shows a series of tensile tests for foam specimens having a density of 0.24 g/cm³. For

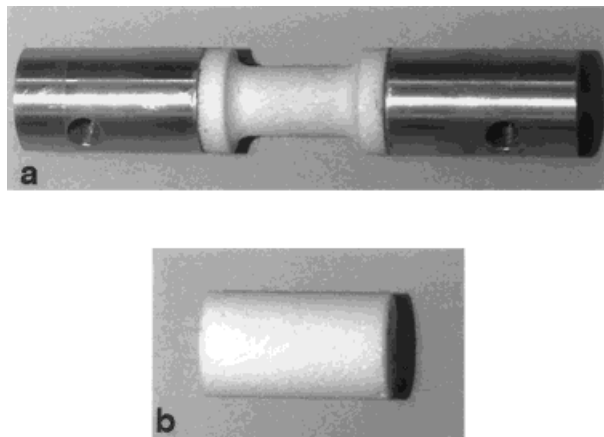


Figure 1 Specimen geometries used in this study: (a) tension specimen had a 25.4-mm gauge length with a 19.0-mm reduced gauge diameter. Steel pull studs were bonded to the specimen ends for mounting in the test frame. (b) Compression specimens were simple, free-standing right cylinders 50.8-mm long and 28.7 mm in diameter.

any given material condition (density), the test results were quite reproducible. The modulus (defined as the initial linear loading portion of the stress–strain curve) for the five tests shown in Figure 3 is 159.0 ± 10.5 MPa. The ultimate tensile strength of the foam is 3.76 ± 0.07 MPa, while the fracture strain is 0.039 ± 0.003 . The energy absorption of this density foam was derived from the area under the stress–strain curves as described above and found to be 0.095 ± 0.012 J/cm³. This general reproducibility was also found for compression testing.

The modulus as a function of foam density is shown in Figure 4. The modulus of the foam exhibits a power-law dependence with respect to the density of the form

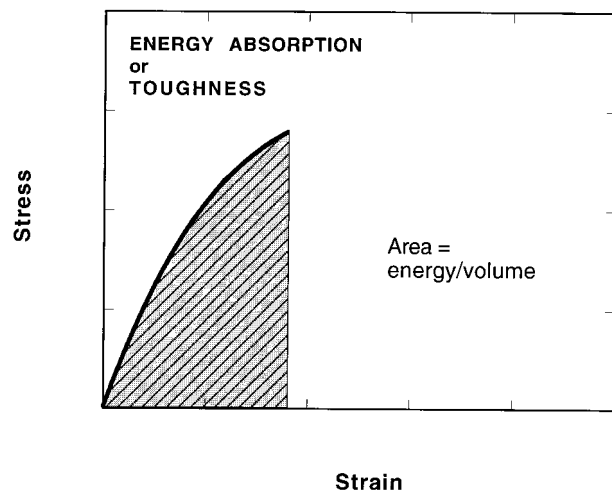


Figure 2 Schematic illustration of the calculation of toughness or energy absorption from either a tension or compression stress–strain curve. The energy absorption is the area under the curve either to the point of failure or to some predetermined strain value.

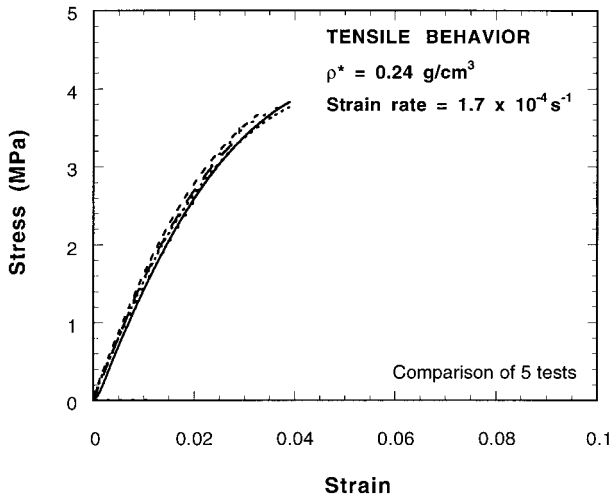


Figure 3 Comparison of five tensile curves for foam specimens, $\rho^* = 0.24 \text{ g/cm}^3$.

$$E^* \propto (\rho^*)^n \quad (1)$$

where E^* is the modulus of the foam, ρ^* is the foam density, and n is the density exponent. It will be shown later that there are sound theoretical reasons to not consider this density exponent as a constant over all possible foam densities. However, over the range of density shown in Figure 4, the data are well fit for a density exponent of $n = 1.6$.

Energy absorption of the material is determined as the area traced out by the stress–strain curves as described earlier. Figure 5 shows the results for the tension testing over the entire range of the foam densities examined. The results

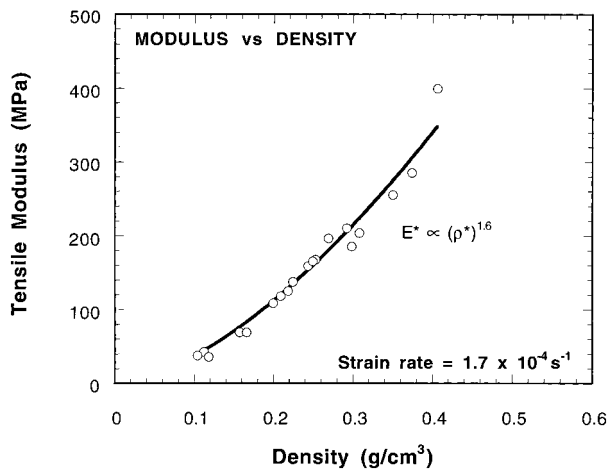


Figure 4 Foam modulus exhibits a power-law dependence with respect to density.

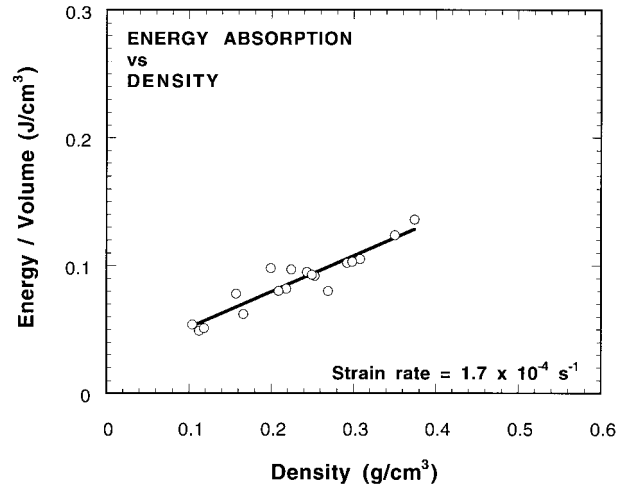


Figure 5 Energy absorption as a function of density for tensile tests. The results indicate that the energy absorption of the material increases linearly with increasing foam density.

indicate that energy absorption of the material increases linearly with increasing foam density. Values range from a low of 0.04 J/cm^3 for foam with a density of 0.104 g/cm^3 to 0.16 J/cm^3 for foam having a density of 0.39 g/cm^3 . It will be shown that the energy-absorption values are quite low compared to the compression-derived values. The energy-absorption values obtained via tensile testing are controlled entirely by the brittle nature and, therefore, the low ductility of the material in tension.

Compression

Figure 3 reveals that the foam is quite brittle in tension—there is little or no macroscopic yielding prior to fracture. Because of the inherent lack of tensile ductility, it is clear that tension testing is not the most appropriate method for evaluating the toughness of a material whose primary mechanical requirement is compressive shock mitigation and energy absorption.

A companion series of compression tests were performed on the material to determine the energy-absorption characteristics under somewhat more realistic conditions. A typical compression test is shown in Figure 6 for a foam having a density of 0.15 g/cm^3 . In compression, the foam specimens show relatively abrupt yielding followed by a sustained plateau region. At the lower densities, such as that shown in Figure 6, the stress after the plateau actually drops, giving rise

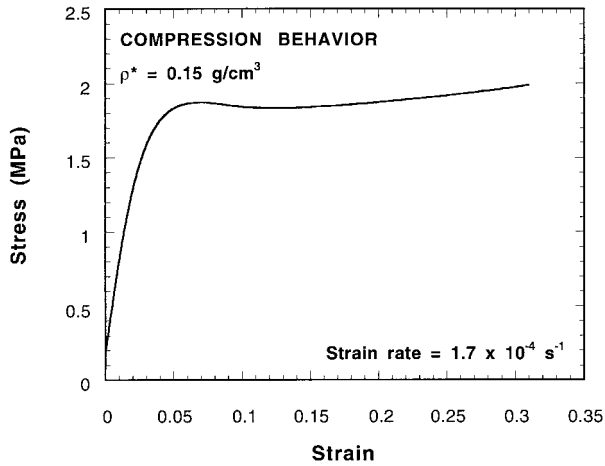


Figure 6 Typical compression test results for a foam having a density of 0.15 g/cm^3 . A relatively abrupt yield point is followed by a sustained plateau region. The stress begins to increase subsequent to this plateau region as the foam begins to densify.

to a yield pointlike behavior. The broad plateau region results from the elastic collapse or cell wall buckling of the foam.¹ The stress begins to increase subsequent to this plateau region as the foam begins to densify. Unlike the tests performed in tension, fracture is inhibited by the absence of tensile stresses, and as a result, engineering strains in excess of 50% have been measured with little observable indication of fracture. To expedite testing, compression strains were limited to 0.3 (30%), which was sufficient to characterize the modulus and plateau stress values for each specimen.

The mechanical properties during the early stages of compression are essentially identical to those observed in tension. Figure 7 compares the tension and compression behavior for a foam having a density of 0.24 g/cm^3 . Both tests were conducted at the same strain rate. The curves overlay up until the point of tensile failure, suggesting that the microstructural processes governing elastic deformation and low strain response in both tension and compression are identical.

The moduli, derived from the compression tests, as a function of foam density are shown in Figure 8. In this figure, the compression moduli are superimposed on the data shown in Figure 4. It is clear that compression testing yields the same moduli as does tensile testing. When all the data are fit to a power-law relationship, the density exponent, n , is still equal to 1.6, as it was for the tension-only moduli in Figure 4.

Figure 9 shows the plateau stress for the foam

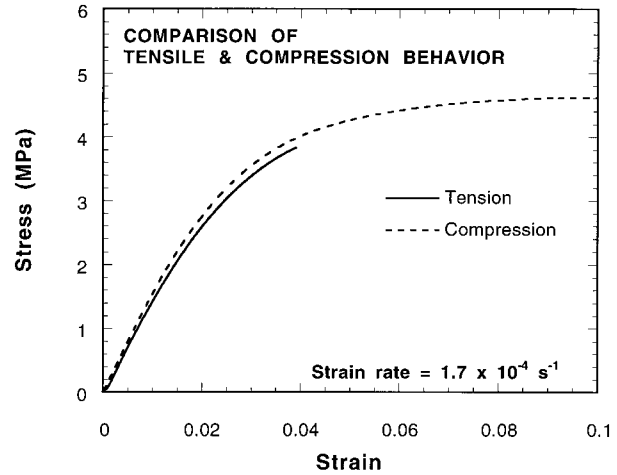


Figure 7 Tension and compression behavior for foam specimens of the same density (0.24 g/cm^3). Compression trace overlays a companion tension test up to the point of tensile failure.

specimens as a function of density. This plateau stress, also called the elastic collapse stress, σ_{el}^* , is important in the design of cushions for shock or impact mitigation as it represents the onset of the mechanical instability of the foam microstructure.¹ It, too, exhibits a power-law dependence with respect to foam density although somewhat higher than the density exponent for the modulus.

The energy absorption of the foam versus density up to the reference strain of 0.1 is shown in Figure 10 along with the data from Figure 5 for tension testing. Values range from a low of 0.10 J/cm^3 for foam with a density of 0.12 g/cm^3 to 1.20 J/cm^3 for foam having a density of 0.495 g/cm^3 . It is clear that the total energy-absorption

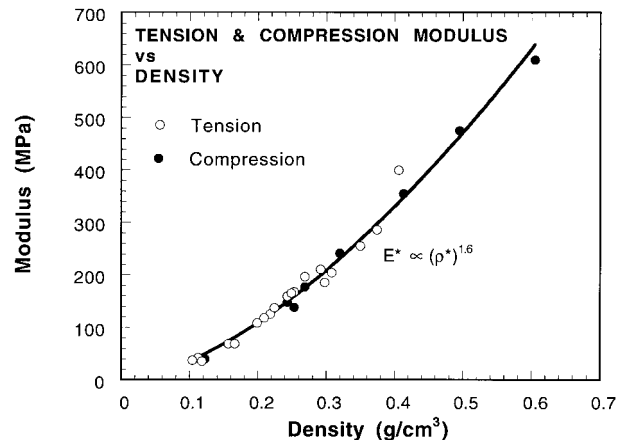


Figure 8 Density dependence of the foam modulus in tension and compression.

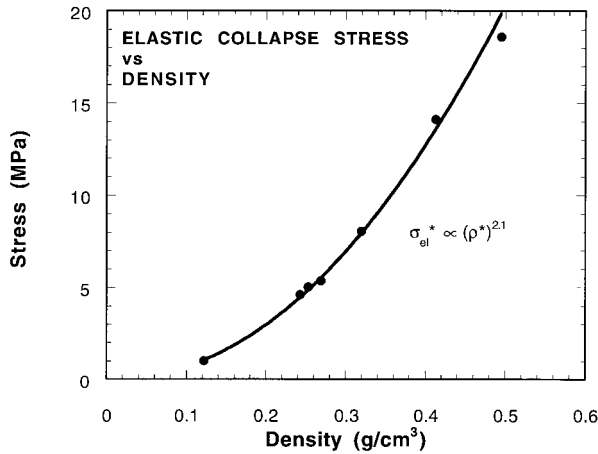


Figure 9 Elastic collapse stress for the foam specimens as function of density. A power-law dependence with respect to foam density is evident.

capacity of the foam in compression far exceeds that in tension for the entire range of density examined. The comparison would be even more striking for energy-absorption values computed at higher reference strains. The difference between the tension- and compression-derived energy values results directly from the inherent brittleness of the material under tensile loading which limits ductility to less than about 0.05 (5%). Because the energy-absorption values in compression are all computed at the constant reference strain of 10%, the relationship between energy absorption and foam density arises directly from the power-law relationship between compressive strength and density as shown in the previous figure.

RELATIONSHIP BETWEEN THE STRUCTURE OF FOAMS AND MECHANICS OF DEFLECTION

The dependence of both the modulus and the elastic collapse stress of a cellular foam can be understood in terms of the mechanical properties of the polymer material from which the cell struts (and in the present case, the cell walls) are made and the deformation mechanics of the cellular structure itself. Elastic moduli are related principally to the bending stiffness of the members composing the cellular structure while the elastic collapse is caused by the elastic buckling of these same members.

For the discussion presented below, the important cell strut/wall properties are the solid

polymer density, ρ_s , and its modulus, E_s . The important structural features for the analysis of the modulus and the collapse stress are the relative density of the foam, ρ^*/ρ_s (as before, ρ^* is the density of the foam) and whether the cells are open or closed. In this regard, a parameter, ϕ , is defined as the fraction of material in the cell struts. For an open-cell foam, $\phi = 1$, while for a closed-cell foam, where some of the polymer is in the cell walls, it is less than 1.

Modulus

Much work has been done over the last 30 years to relate the mechanical response of foams to the mechanics of cell deformation. Gibson and Ashby¹ have done an extensive review of this earlier work and have shown that, in many cases, attempts to describe the mechanical properties of cellular solids analytically have been based on incorrect assumptions. In a number of instances, the axial extension of cell struts has been used to describe the low strain behavior of foams^{2,3} even though it is the bending stiffness of the struts that principally controls small strain deformation. For example, Gent and Thomas² based their analysis on a cell structure that requires tensile moduli to be governed by the extension of struts lying parallel to the tensile axis while compression moduli are governed by the buckling of these same struts. We have shown that the tension and compression curves for the rigid CRETE foam system overlay

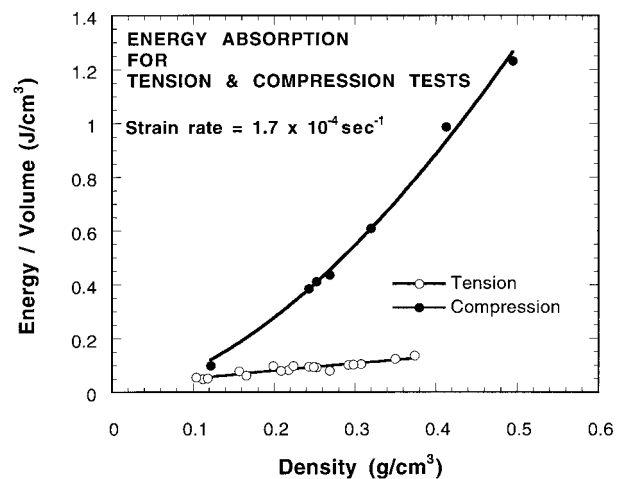


Figure 10 Energy absorption of the foam versus density along with the data from Figure 5 for tension testing. The energy-absorption capacity of the foam in compression far exceeds that in tension for the entire range of density examined.

up until the point of tensile failure (Fig. 7), strongly suggesting that the processes governing deformation are independent of the sign of the applied stress. This observation is inconsistent with the premise put forth in ref. 2. Others described the elastic behavior of foams in a manner that requires that the cell struts of the foam be initially bent, leading to results that do not have general applicability.^{4,5}

The principal mechanism of linear-elastic deformation for foams was first identified correctly by Menges and Knipschild as cell wall bending.⁶ They also pointed out that open- and closed-cell foams have similar stiffness because it is the cell wall edges or struts, rather than the thin cell wall membranes, that carry the majority of an imposed load. Ko also identified cell wall bending as the controlling factor in the determination of the modulus, but the model presented in that work is complicated by the extremely complex cell geometry.⁷ Similarly, Patel and Finnie reported in great detail the geometrical requirements necessary for various three-dimensional structures to fill space.⁸ Their work was predicated on the fact that as a foam expands the bubbles or spheres which compose it impinge to form polyhedra. They describe how no regular polyhedra can meet all of the angular requirements for mutually shared edges while satisfying compatibility (i.e., that the repeated polyhedron fills all space with no void). The only structure that meets all geometric requirements is the "minimum area tetrakaidecahedron" having 109.47° angles between adjoining pairs of cell edges and having hexagonal faces of double curvature. Analysis of the mechanics of a cell structure based on such a unit cell leads to intractable mathematics. The authors attempted to simplify their analysis by using a pentagonal dodecahedron which approximately satisfies the geometry and compatibility requirements. However, even this simplification leads to an extremely complex analysis that is difficult to apply generally.

A much simplified model of an open-cell foam was put forth by Gibson and Ashby⁹ in which the foam is modeled as an array of cubic cells of length, l , and struts of thickness, t , as shown in Figure 11. The cells are then staggered so that the corners of one cell rest upon the midpoint of adjacent cells. Such a structure neither corresponds to the actual geometric characteristics of a real foam nor can be reproduced to fill space. This "unit cell" does, however, capture the critical physical processes that govern the deformation

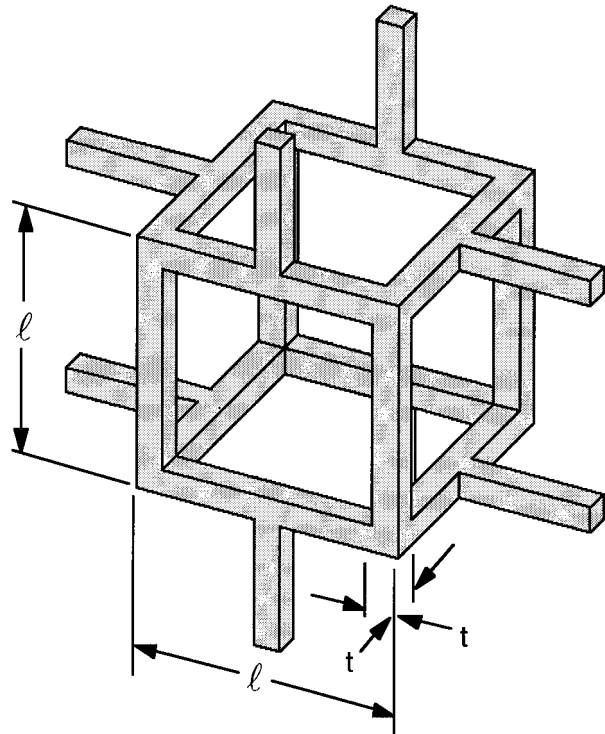


Figure 11 Unit cell for an open-cell foam of cubic symmetry. The cell is composed of edges or struts of length l and thickness t .

and structural stability of a cellular solid. Defined in this manner, the volume of the material in each strut is

$$V_{\text{strut}} = t^2l \quad (2)$$

Since each strut is shared by a maximum of three adjoining cells, the relative volume of material in each cell is

$$V^* \geq \frac{12}{3} t^2l \quad (3)$$

The relative density of such a foam structure is related to the cell dimensions as

$$\frac{\rho^*}{\rho_s} \propto \frac{V^*}{V_c} \propto \left(\frac{t}{l}\right)^2 \quad (4)$$

where V_c is the cell volume, l^3 .

The elastic modulus of the cellular structure can be calculated from the elastic deflection of a beam of length l loaded at its midpoint by a load

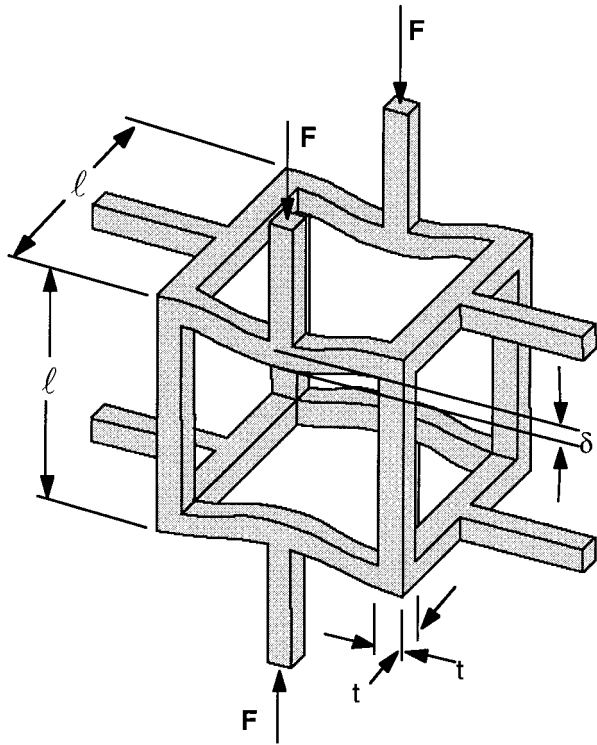


Figure 12 Unit cell shown after linear-elastic deflection of magnitude δ induced by a force F .

F , as shown in Figure 12. Beam theory¹⁰ gives this deflection, δ , as

$$\delta \propto \frac{Fl^3}{E_s I} \quad (5)$$

where $I \propto t^4$ is the moment of inertia of the point-loaded strut. When a uniaxial remote stress is applied to the foam so that each strut sees a transmitted force equal to F , the entire structure then suffers an elastic deflection given by eq. (5). The remote stress, σ , is proportional to F/l^2 and the overall strain, ε , scales with the cell dimensions as δ/l . The modulus of the foam therefore is given as

$$E^* = \frac{\sigma}{\varepsilon} = \frac{C_1 E_s I}{l^4} \quad (6)$$

where C_1 contains all the geometric constants. Since a foam is not composed of a completely uniform cell geometry and size, it is more appropriate to determine the value of C_1 by fitting eq. (6) to data rather than solving for it analytically. Gibson and Ashby^{1,9} fit eq. (6) to the modulus measure-

ments for a wide range of materials and showed that $C_1 \approx 1$. Using eq. (4) and substituting for I ,

$$\frac{E^*}{E_s} \approx \left(\frac{t^4}{l^4}\right) \approx \left(\frac{\rho^*}{\rho_s}\right)^2 \quad (7)$$

Equation (7) describes the density dependence of the elastic modulus of an open-cell foam only at small displacements. As strains increase and the loading on the struts parallel to the applied force approaches the Euler load, buckling occurs. Under these conditions, deflection is no longer linear with increasing stress and eq. (7) no longer applies. However, at low strains where the additional moments induced by Euler buckling can be ignored, eq. (7) is valid and is applicable to tensile loading as well.

Equation (7) predicts that, at low strains, a parabolic relationship exists between the modulus of the foam and its density. The data in Figure 8, however, suggest that the power-law exponent is less than 2. This discrepancy can be found in the fact that the polyurethane CRETE is a closed-cell foam rather than an open-cell foam. In deriving eq. (7), it is assumed that all the material of the foam is found in the struts that define the cells. In a closed-cell foam, some fraction of the polymer resides in the cell walls or faces rather than in the struts (see Fig. 13).

If the fraction of polymer contained in the cell struts having thickness t is ϕ , then the fraction contained in the cell walls of thickness t_f is $(1 - \phi)$. The stiffness of a closed-cell foam results then from three contributions: The first component is strut bending, as for open-cell foams. The second component is membrane (cell face) stretching^{8,11} which arises as the result of strut flexure causing the cell walls to deform. The final component is the internal gas pressure of the closed cells.

Gibson and Ashby^{1,9} derived the modulus of a closed-cell foam which accounts for all three components:

$$\frac{E^*}{E_s} \approx \phi^2 \left(\frac{\rho^*}{\rho_s}\right)^2 + (1 - \phi) \frac{\rho^*}{\rho_s} + \frac{p_0(1 - 2\nu^*)}{E_s(1 - \rho^*/\rho_s)} \quad (8)$$

The first term on the right describes the contribution of the cell struts to the modulus while the second term accounts for the cell walls. The third term is the contribution due to the internal gas pressure, where ν^* is Poisson's ratio for the foam.

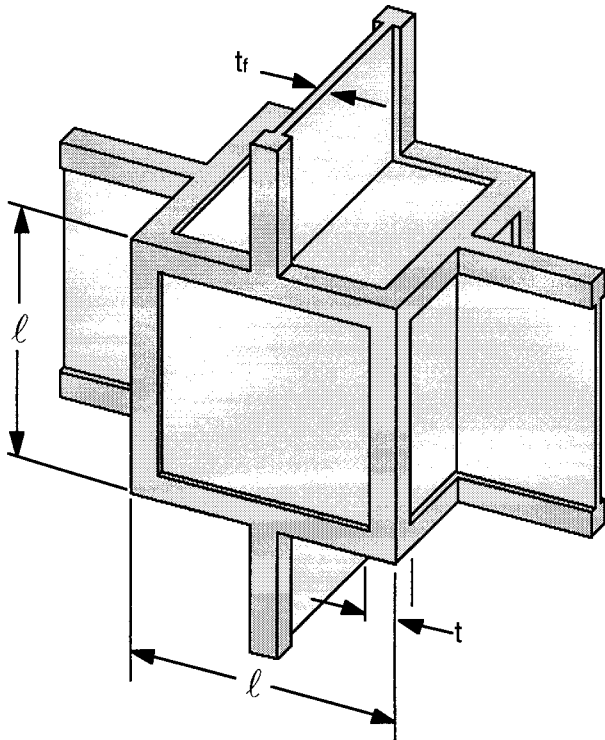


Figure 13 Unit cell for a closed-cell foam of cubic symmetry. The cell is composed of edges or struts of length, l , and thickness, t . Cell faces are closed by membranes of thickness t_f .

When p_0 is small, gas pressure effects are negligible, as is the current situation. Equation (8) then becomes

$$\frac{E^*}{E_s} \approx \phi^2 \left(\frac{\rho^*}{\rho_s} \right)^2 + (1 - \phi) \frac{\rho^*}{\rho_s} \quad (9)$$

Note that eq. (9) reduces to eq. (7) for $\phi = 1$ (an open-cell foam). The form of eq. (9) is such that at high relative densities the modulus varies as the square of the density, while at low relative densities, the modulus is more nearly linearly dependent on the density. Within these density extremes, eq. (9) yields a power-law relationship which can describe the functional dependence of the modulus on density with an exponent of 1.6, the value that best fits the data shown in Figure 8.

The data shown in Figure 8 can be directly compared to eq. (9) using known values for ρ_s and E_s . This comparison is shown in Figure 14 for $\phi = 0.9$. (Note that we have not independently measured ϕ for this foam system; the value used, $\phi = 0.9$, is typical for polyurethane foams.¹²) For the density

of the solid, we used a value of 1.2 g/cm^3 .¹³ The value for the modulus of solid polyurethane is less well established and varies considerably depending on the precise formulation, processing conditions, and product form. Data in the literature suggest that a reasonable range for the modulus of the solid is between 1.6 and 2.7 GPa.^{8,13,14} These two values are used to bound the dependence of the modulus on the foam density predicted by eq. (9). It is clear from Figure 14 that the model well represents the data over the range of densities examined experimentally.

Elastic Collapse

The dependence of the plateau stress on foam density was also addressed by Gibson and Ashby.^{1,9} When a cellular solid is loaded in compression, the cell walls first flex, as shown in Figure 12. When the vertical load in Figure 12 is small, the compressed columns that comprise the cell struts parallel to the applied load are laterally stable. Indeed, small transverse displacements tend to self-correct and the column returns to a position aligned with the loading direction. As the load is increased, the column becomes unstable and lateral displacements tend to remain. This instability is termed "lateral buckling" and the applied load necessary to cause it is called the "Euler buckling load." The derivation of the Euler buckling load is a well-known problem in mechanics.¹⁵ For a slender column of a constant cross section, pinned at each end and subjected to axial compression, it is given by

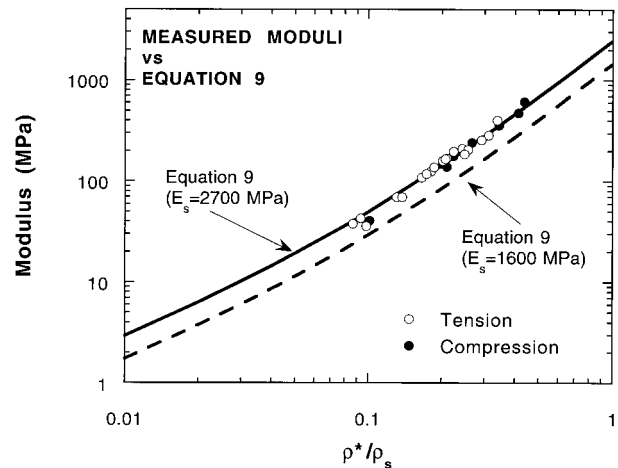


Figure 14 Comparison of modulus measurements to eq. (9). Note that density is normalized to the density of the solid polymer.

$$F_{\text{crit}} = \frac{\pi^2 E_s I}{l^2} \quad (10)$$

When this load is reached, a layer of cells in a compression specimen will buckle, initiating elastic collapse. The stress at which this happens, σ_{el}^* , is given by

$$\sigma_{el}^* \propto \frac{F_{\text{crit}}}{l^2} \propto \frac{E_s I}{l^4} \quad (11)$$

Using previously defined relationships, the elastic collapse stress for cellular foam is defined as

$$\frac{\sigma_{el}^*}{E_s} = C_2 \left(\frac{\rho^*}{\rho_s} \right)^2 \quad (12)$$

where C_2 again contains all of the proportionality constants. Note that the cell walls in a closed-cell foam contribute little to buckling resistance so that no modifications to eq. (12) are necessary.

However, the densification of the material does affect the buckling characteristics. Gibson and Ashby⁹ refined eq. (12) to account for density effects and reported slightly modified results (ignoring internal gas pressure):

$$\frac{\sigma_{el}^*}{E_s} = C'_2 \left(\frac{\rho^*}{\rho_s} \right)^2 \left[1 + \left(\frac{\rho^*}{\rho_s} \right)^{1/2} \right]^2 \quad (13)$$

The correction for density is negligible when ρ^*/ρ_s is less than 0.3, but has the effect of making the foam more resistant to collapse at higher density. To obtain a quantitative comparison to the data shown in Figure 10, the value of C'_2 must be determined. By fitting eq. (13) to data in the literature for polyurethane, polyethylene, and latex rubber, Gibson and Ashby^{1,9} determined that $C'_2 = 0.03$. We used this independently determined value for C'_2 and the same values for ρ_s and E_s , as used before, to compare the elastic collapse stress measurements in Figure 9 to eq. (13). The results are shown in Figure 15.

Notwithstanding the uncertainty in some of the parameters, the agreement between the measured and predicted elastic collapse stress is quite good. Equation (13) predicts both the density dependence of σ_{el}^* as well as quantitatively predicting the actual measured values.

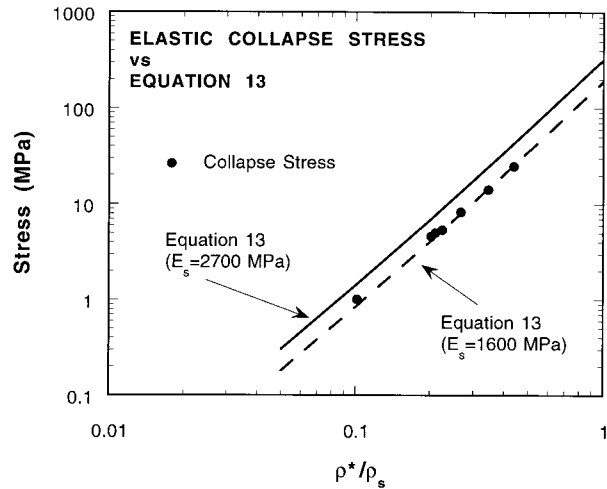


Figure 15 Comparison between the measured elastic collapse stress and eq. (13).

Energy Absorption

Toughness is essentially the product of both strength and ductility as described in the Experimental section. Thus, to effectively predict the energy absorption of foams, it is necessary to develop a model that relates the *strength* of the foam to the mechanics of deflection (as presented above for both modulus and elastic collapse stress) and also relates the *failure strain* of the foam to the intrinsic ductility of the polymer material and/or to the foam structure. With respect to the latter consideration, no such model currently exists. Such an effort is made difficult by the fact that, for many polymeric foam systems, certain properties of the bulk polymer such as ductility may not be comparable to the properties of the polymer as it exists in the struts or walls of a cellular structure. Differences arise from a variety of factors including the fact that the blowing action that occurs during the processing of a foam induces strain and directionality in the cell struts, neither of which will exist in a monolithic bulk polymer.

Other difficulties arise when trying to reproduce the bulk polymer itself. In the present case, water is the blowing agent but it also participates in the chemistry of the polyurethane reaction. Removing it from the formulation will result in a polymer of fundamentally different chemistry and structure. Yet another difficulty arises with respect to the heat generated by the reaction of the polyol and isocyanate. The isocyanate tends to boil and form pores within the "solid" polymer even if water is removed from the formulation. Such pores acting as stress concentrators can signifi-

cantly reduce the ductility of the polymer. This pore formation can be suppressed by removing the surfactant in the formulation but this further alters the chemistry of the polymer, yielding a material whose relationship to the polyurethane in the foam is uncertain.

CONCLUSIONS

Energy-Absorption Characteristics of the Foam System

The data presented in the Results and Discussion section clearly indicate that the toughness or energy-absorption characteristics of the foam are dependent on the test methods employed. The susceptibility of these foams to tensile failure results in the lowest computed values of toughness of any of the measurement schemes examined in this study. We conclude, therefore, that because these foams are inherently brittle the use of tensile testing to characterize their shock mitigation qualities is inappropriate as it yields the least representative values for energy absorption. Compression testing, while somewhat more realistic in terms of loading characteristics, does not capture the intrinsic limitations in the material under dynamic or impact loading conditions. High-density specimens can be deformed to engineering strains of > 50%. Low-density specimens⁹ can be deformed in excess of 80% without any macroscopic indication of mechanical failure. As such, the energy values determined from compression testing must be determined at some arbitrarily defined reference strain and are therefore not indicative of intrinsic material performance. Additional work is in progress that will assess the energy-absorption characteristics under more representative impact conditions.

Structure Dependence of Modulus and Collapse Stress

The agreement between the measured modulus and the collapse stress with those predicted by eqs. (9) and (13) suggests that the models put

forth in the literature^{1,9} based on simple, idealized cell geometries can be useful in describing certain important mechanical and physical properties of encapsulant foams. The agreement is remarkable in light of the straightforward unit cell geometries chosen as the basis of the model. While not physically realistic, these cell geometries capture the physical processes upon which the cellular solid properties are dependent. In this regard, it is clear that the modulus is dependent upon the flexure of cell struts while the elastic collapse stress is dependent upon cell edge buckling.

This work was supported by DOE Contract DE-AC04-94AL85000.

REFERENCES

1. L. J. Gibson and M. F. Ashby, *Proc. R. Soc. A*, **382**, 43 (1982).
2. A. N. Gent and A. G. Thomas, *J. Appl. Polym. Sci.*, **1**, 107 (1959).
3. J. M. Lederman, *J. Appl. Polym. Sci.*, **15**, 693 (1971).
4. R. Chan and M. Nakamura, *J. Cell. Plast.*, **5**, 112 (1969).
5. Barma, M. B. Rhodes, and R. Salovey, *J. Appl. Phys.*, **49**, 4985 (1978).
6. G. Menges and F. Knipschild, *Polym. Eng. Sci.*, **15**, 623 (1975).
7. W. L. Ko, *J. Cell Plast.*, **1**, 45 (1965).
8. M. R. Patel and I. Finnie, *J. Mater.*, **5**, 909 (1970).
9. L. J. Gibson and M. F. Ashby, *Cellular Solids, Structure and Properties*, Pergamon Press, New York, 1988.
10. S. Timoshenko and D. H. Young, *Elements of Strength of Materials*, 4th ed., D. van Nostrand, New York, 1962.
11. D. J. Green, *J. Am. Ceram. Soc.*, **68**, 403 (1985).
12. D. W. Reitz, M. A. Schuetz, and L. R. Glicksman, *J. Cell. Plast.*, **20**, 104 (1984).
13. W. F. Roff and J. R. Scott, *Fibres, Films, Plastics and Rubbers—A Handbook of Common Polymers*, Butterworths, London, 1971.
14. *Plastics Digest*, Vol. 2, D.A.T.A., Englewood, CO, 1994, pp. 1301–1304.
15. W. A. Nash, *Strength of Materials*, 3rd ed., Schaums Outline Series, McGraw-Hill, New York, 1994.